SLIIT International Conference on Engineering and Technology
Malabe, Sri Lanka, September 2025

A Numerical Investigation of the Potential of Dimpled Surface Configurations to Improve Aerodynamic and Aeroacoustic Performance of Airfoils

Nisal Nelaka Fernando[1, a *], Indrajith Nissanka[2, b] and Nalaka Samaraweera[3, c]

[1,2,3]Department of Mechanical Engineering, Faculty of Engineering, University of Moratuwa, Moratuwa 10400, Sri Lanka

[a]fernandoinn.24@uom.lk, [b]nissankai@uom.lk, [c]nalakas@uom.lk

KEYWORDS: *Dimpled Airfoil; Aerodynamics, Aeroacoustics, Cfd, Naca 0012, Detached Eddy Simulations (Des), Passive Flow Control*

ABSTRACT

This study investigated the potential of dimpled surface configurations to enhance the aerodynamic and aeroacoustic performance of airfoils. Computational Fluid Dynamics (CFD) simulations were carried out on a NACA 0012 airfoil featuring surface dimples, under flow conditions relevant to low-speed aerodynamic applications such as unmanned aerial vehicles (UAVs), light aircraft, and small-scale wind turbines. The simulations were conducted at a Reynolds number of 700,000 and a Mach number of 0.21, representing typical subsonic operating conditions. Two angle of attack, 5° and 10°, were examined to represent attached flow and near-stall behavior, respectively. Aerodynamic performance was evaluated through lift and drag coefficients, while aeroacoustic characteristics were analyzed using Overall Sound Pressure Level (OASPL) with directivity plots and frequency spectrum analysis based on the Ffowcs Williams–Hawkings (FW-H) acoustic analogy. Key findings indicate that the dimpled configuration enhances flow behavior by increasing lift and reducing drag at a 10° Angle of Attack (AoA), primarily through delayed separation and modified stall onset characteristics. Aeroacoustic analysis showed a noise reduction of 2–7 dB at various receiver positions at a 10° AoA, with reductions varying by observer angle and frequency, confirming the directional sensitivity of noise emissions. These insights contribute to the understanding of passive flow control mechanisms and their dual impact on aerodynamic performance and noise reduction in airfoil design

INTRODUCTION

Aeroacoustic noise generated by turbulent fluid flow and unsteady aerodynamic forces, has become a growing concern in many low-speed aerodynamic applications such as small-scale unmanned aerial vehicles (UAVs), wind turbines, and industrial fans. This form of noise not only impacts human health and comfort but also affects the surrounding environment by interfering with wildlife communication and behavior [13]. Regulatory bodies such as the Federal Aviation Administration (FAA) and the Environmental Protection Agency (EPA) have responded by implementing strict noise limitations often below 65 dB for residential zoning near airfields [9] and 52 dB for wind energy installations, depending on land use and frequency [6]. As a result, the demand for passive noise reduction technologies has increased significantly.

Simultaneously, maintaining or improving aerodynamic performance remains essential, as any noise reduction strategy that leads to increased drag or reduced lift may offset its practical value. An increase in drag leads to higher energy consumption, while reduced lift can compromise efficiency or system capability. Therefore, there is a strong need for passive flow control techniques that can address both aerodynamic and acoustic concerns without introducing complex structural changes.

Dimples, which are shallow, concave surface features, have emerged as a promising passive flow control strategy in airfoils. By promoting localized turbulence, dimples help re-energize the boundary layer, potentially delaying flow separation and enhancing lift during low-speed operation. Unlike traditional vortex generators, which often involve protruding elements that can increase drag at higher speeds and complicate the surface structure [11,12], dimples provide a flush configuration that is easier to manufacture and maintain. However, the turbulent structures induced by dimples can also influence the aeroacoustic characteristics of the surface, either positively [18] or negatively, depending on their configuration and flow conditions [19]

https://doi.org/10.54389/LCXD9652

While many studies have explored the aerodynamic effects of dimples mainly on flat plates at low Reynolds numbers [7,14,16], very few have investigated their combined aerodynamic and aeroacoustic performance on airfoils at moderate Reynolds numbers suitable for small UAVs, Wind Turbines and small Aircraft, Ananthan et al. (2022) [2] investigated a shallow dimple configuration at zero angle of attack and reported a drag increase of 1.9% with no detailed acoustic analysis. To the best of the author's knowledge, no comprehensive study has been conducted to examine how dimple geometry influences both lift–drag characteristics and noise generation across multiple angles of attack at Reynolds numbers relevant to real-world applications.

This study aims to investigate the influence of dimpled surface configurations on both aerodynamic and aeroacoustic performance of airfoils, focusing on low-speed applications such as UAVs, small wind turbines, and light aircraft operating at a Reynolds number of approximately 700,000. The objectives are to evaluate the lift–drag characteristics, analyze the noise reduction potential, and correlate flow structures with changes in aerodynamic and aeroacoustic performance. To achieve these, Computational Fluid Dynamics (CFD) simulations were conducted on a selected airfoil profile with dimple arrangements and different angles of attack. The results provide insights into the dual impact of dimpled surfaces on performance and noise, supporting their feasibility as a passive flow control method for broader low-speed aerodynamic applications.

METHODOLOGY

Geometry and Dimple Configuration

The NACA 0012 airfoil was selected for this investigation due to the extensive availability of high-quality experimental aerodynamic and aeroacoustic data at Reynolds numbers around 700,000, its symmetrical geometry, and its widespread use as a benchmark in CFD-based aerodynamic and aeroacoustic studies. The airfoil had a chord length of 150 mm and a span of 450 mm (3c), forming a quasi-2D configuration to isolate mid-span aerodynamic and aeroacoustic behavior while minimizing computational cost. This approach aligns with prior studies, which identify turbulent boundary layer trailing-edge noise and separation-induced stall noise at the mid-span as dominant contributors for low-speed airfoils (Figure 1(a)).

A semi-spherical dimple configuration was introduced on the suction side of the airfoil as shown in the Figure 1(b). Each dimple had a diameter of 5 mm, equivalent to 3.3% of the chord, which falls within the range (2%–7%) found effective in prior aerodynamic studies [4,5]. The dimples were arranged starting at 53% of the chord and continued up to 80%, distributed in five longitudinal rows to influence boundary layer behavior beyond mid-chord an area prone to early flow separation at higher angle of attack.

The use of semi-spherical dimples was preferred over hexagonal or rectangular geometries because of their balance between drag performance and noise reduction. While hexagonal dimples offered slightly better drag reduction (~1.2%), semi-spherical ones consistently demonstrated superior aeroacoustic behavior, particularly in low to moderate Reynolds number regimes [3,17]. Moreover, rectangular dimple patterns were found to generate more turbulent structures and less stable flow patterns [8], making them less suitable for passive noise control strategies.

This configuration aimed to improve aerodynamic performance by maintaining attached flow and simultaneously reducing turbulent noise without requiring significant structural modification making it practical for aerospace and wind energy applications where minimal geometric alteration is preferred.

Flow and Boundary Conditions

The simulations were conducted at a freestream Mach number of 0.21, corresponding to a chord-based Reynolds number of 700,000, calculated using a standard speed of sound of 340 m/s. This Reynolds number was selected as it falls within the typical mid-span operating range of UAVs, small wind turbines, and light aircraft. Two angles of attack were considered: 5° to represent attached-flow conditions, and 10° to represent pre-stall conditions. These choices align with aerodynamic performance regimes commonly studied for such low-speed applications

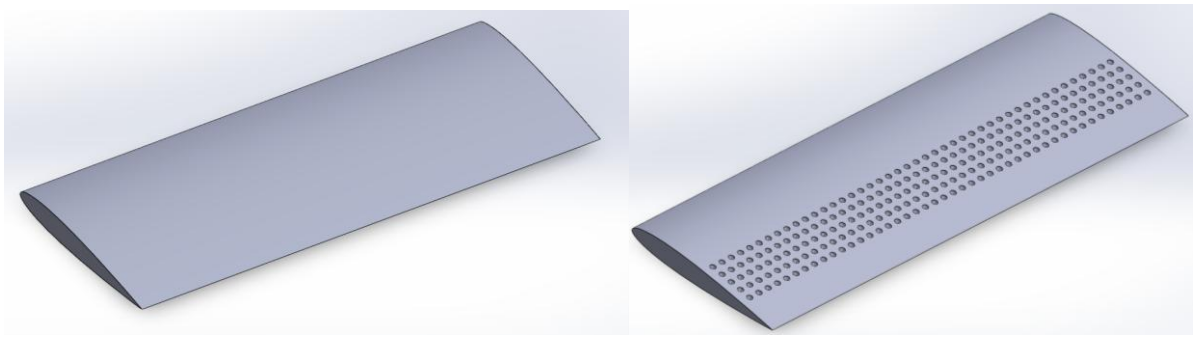

(a) (b)

Figure 1. NACA 0012 Computer Aided Model (a)Clean Wing (b)Dimpled Wing

Computational Domain and Meshing

A quasi-2D computational domain was used, extending 6c upstream and 12c downstream of the airfoil. A polyhedral mesh was adopted to accurately capture surface curvature, with local refinement applied in the dimple regions. Near-wall prism layers were included to maintain y+<1 around the dimples, ensuring adequate resolution of the boundary layer. Each 5 mm dimple was resolved with at least 20 elements across its diameter to capture the relevant flow features. A mesh sensitivity study was conducted to establish the optimum mesh density for both aerodynamic and aeroacoustic predictions. As shown in Figure 2, no significant differences in Cl and Cd were observed beyond 1.4 million elements. Therefore, a final mesh with approximately 1.4 million polyhedral elements was used, as depicted in Figure 3.

A velocity inlet was defined with a magnitude of 71.3 m/s to match the desired Mach number. The outlet was set as a pressure outlet with ambient pressure conditions. The airfoil surface was treated as a no-slip wall, while the remaining domain boundaries were specified as symmetry planes to reduce computational cost and simulate a quasi-2D flow environment.

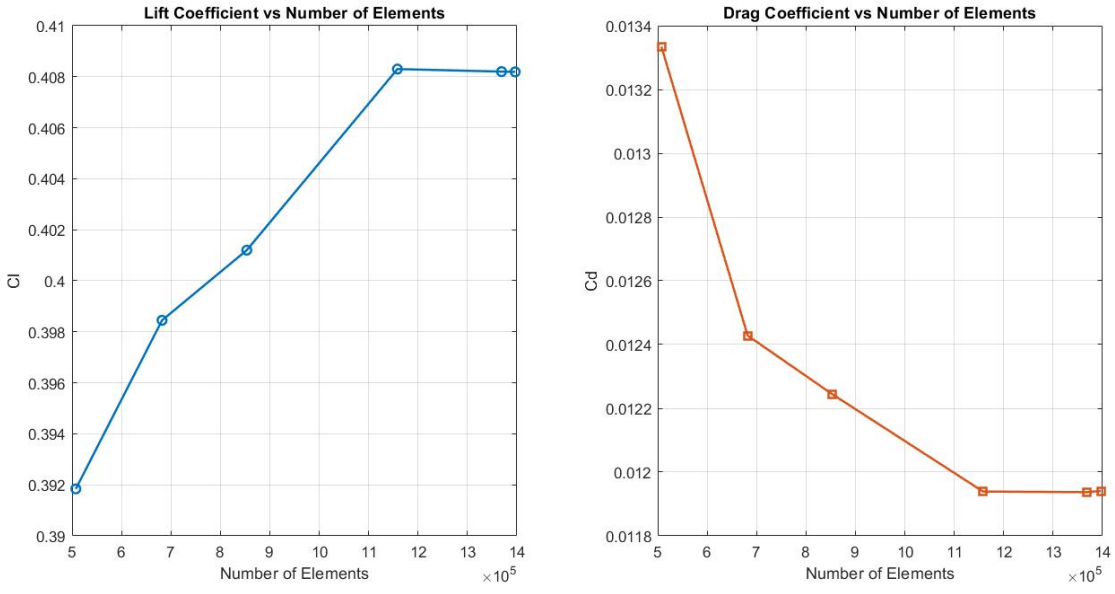

Figure 2. Mesh Independence Study

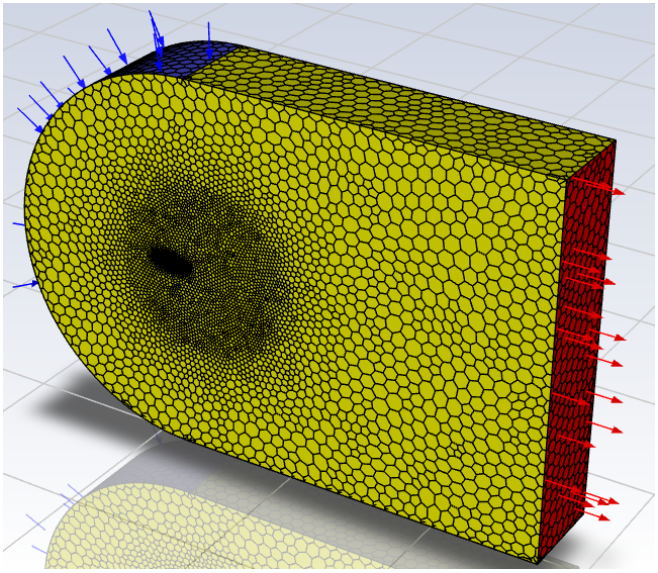

Figure 3. Computational Mesh with Polygonal Elements

Turbulence Model and Acoustic Model

A hybrid turbulence modeling approach was adopted using the Delayed Detached Eddy Simulation (DDES) model based on the SST k-ω formulation, offering improved accuracy in capturing unsteady flow structures critical for aeroacoustic.

For the aeroacoustic analysis, the FW-H equation was employed to predict sound propagation in the far field. The FW-H formulation is an extension of Lighthill's acoustic analogy and is well-suited for compressible, turbulent flows involving solid boundaries. It allows for the calculation of noise generated by both volume sources (turbulence) and surface sources (airfoil motion and pressure fluctuations) [10]. This method is widely followed for aeroacoustic studies due to its ability to decouple the sound generation mechanisms from the propagation effects, enabling efficient post-processing of CFD results to obtain far-field acoustic metrics.

In this study, the permeable FW-H formulation was used, allowing integration over a virtual surface surrounding the airfoil. This approach is particularly advantageous when simulating unsteady flows using hybrid turbulence models such as DDES, as it captures transient pressure fluctuations that are directly linked to acoustic emission mechanisms.

Aerodynamic and Acoustic Validation

To assess the accuracy of the CFD model, the aerodynamic results were validated against experimental data from Sheldahl and Klimas (1981) [15], who tested the NACA 0012 airfoil at a Reynolds number of 700,000. The comparison was carried out for lift and drag coefficients across varying angle of attack. The simulated Cl and Cd values showed strong agreement with the experimental trends, particularly in the linear region. A slight deviation observed around an angle of attack of 10°, which is near the stall onset, is attributed to the simulation approach used at this condition. At higher angle of attack, the flow becomes unsteady due to the formation of vortex bubbles, which causes fluctuations in Cl and Cd. To obtain stable, time-averaged aerodynamic coefficients for comparison with experimental data, steady-state RANS (Reynolds-Averaged Navier–Stokes) simulations were used at these angles. In contrast, Detached Eddy Simulation (DES) was employed in the rest of the study to capture unsteady flow behavior and perform aeroacoustic analysis. This difference in modeling approach may have contributed to the localized discrepancy seen in the aerodynamic validation.

To validate the acoustic model, the computed SPL spectrum at Re = 700,000 for the NACA 0012 airfoil was compared with experimental data from Al Tlua et al. (2021) at Re = 500,000. Despite differences in Reynolds number, chord length, and receiver location, the comparison focuses on overall spectral trends rather than absolute SPL values (Figure 5). Both datasets show a similar broadband decay in SPL with increasing frequency and lack tonal peaks, indicating the simulation captures key noise-generation mechanisms. Prior studies [20,21] confirm that broadband trailing-edge noise spectra remain consistent across moderate Reynolds number changes under low-Mach conditions. Thus, the qualitative agreement supports the DES–FW-H approach as a reliable method for

predicting airfoil noise in such regimes.

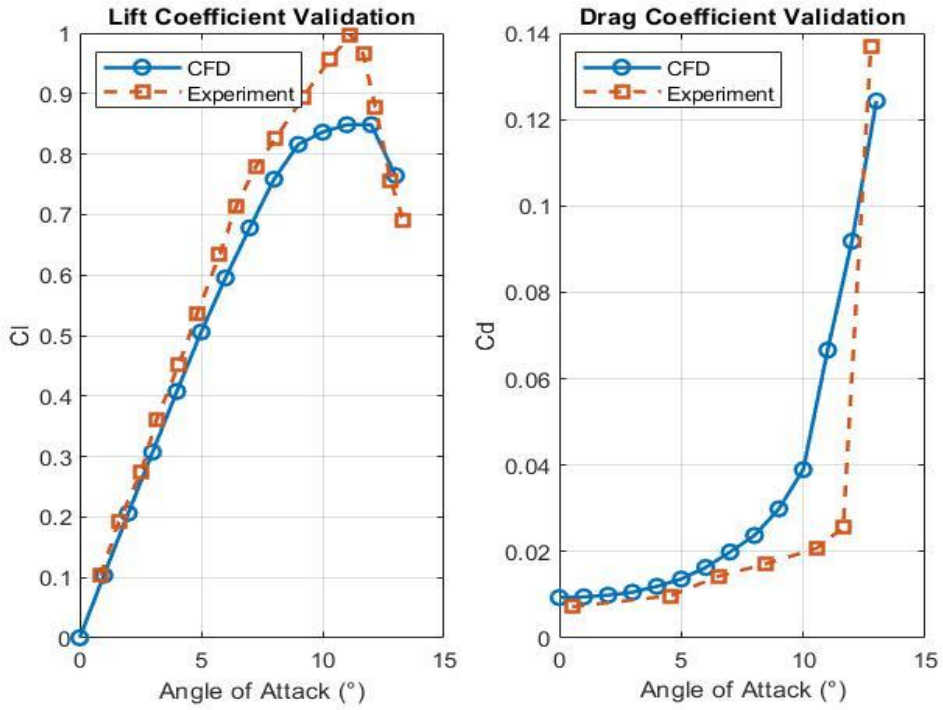

Figure 4. Aerodynamic Validation Cl vs AoA and Cd vs AoA curves

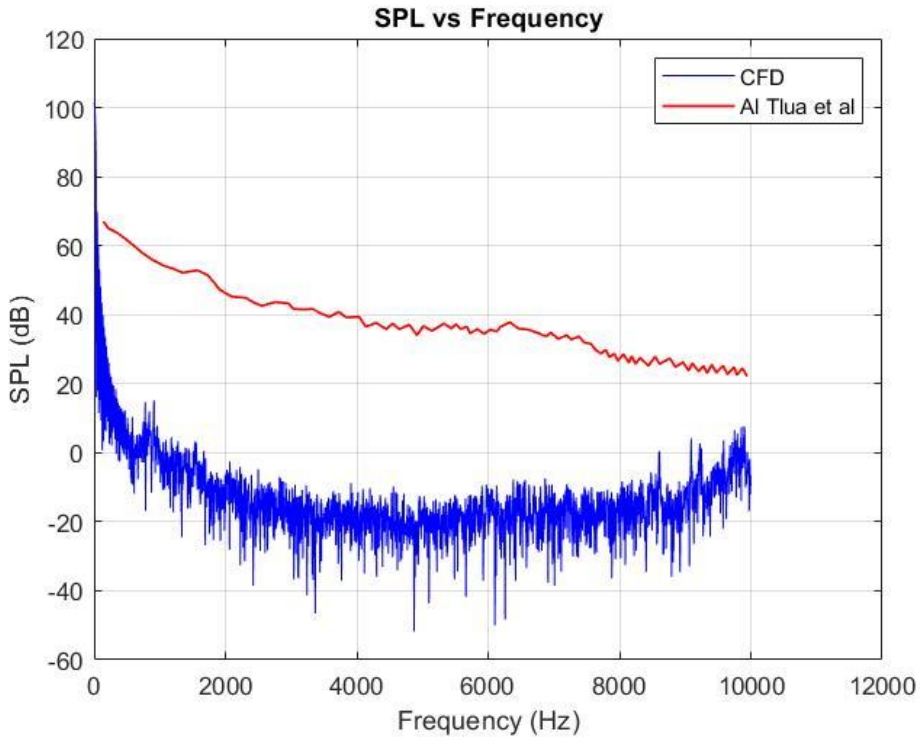

Figure 5. Acoustic Validation: SPL vs Frequency of CFD and Experimental Study

RESULTS AND DISCUSSION

Aerodynamic Performance

For aerodynamic performance evaluation, lift coefficient (Cl), drag coefficient (Cd), and lift-to-drag ratio (Cl/Cd) were extracted for both the clean and dimpled NACA 0012 airfoils at angle of attack 5° and 10°. Velocity and pressure contours were also generated, however no significant differences between the configurations were observed. Therefore, wall shear stress plots and Q-criterion iso-surfaces were presented to visualize the near-wall

behavior and vortex structures in the simulated scenario.

Table 1. Cl, Cd, Cl/Cd vs AoA of Clean and Dimpled Wings

	AoA (degrees)	**Cl**	**Cd**	**Cl/Cd**
Clean Wing	5	0.49	0.0174	28.13
Dimpled Wing	5	0.48	0.0178	26.79
Clean Wing	10	0.84	0.0489	17.07
Dimpled Wing	10	0.86	0.0415	20.74

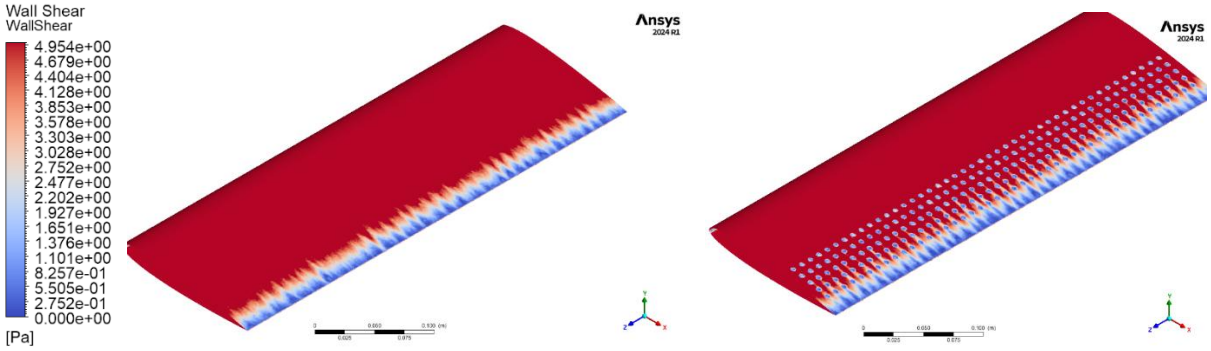

(a) (b)

Figure 6. Wall Shear at AoA $\mathbf{5}^0$ (a) Clean Wing (b) Dimpled Wing

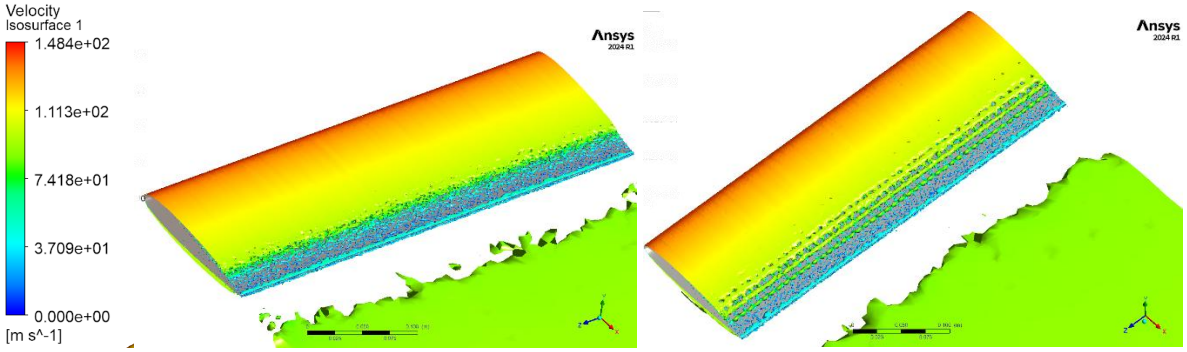

(a) (b)

Figure 7. Q Criterion Iso-surface at AoA $\mathbf{5}^0$ (a) Clean Wing (b) Dimpled Wing

At an angle of attack of 5°, the clean wing produced a lift coefficient (Cl) of 0.49 and a drag coefficient (Cd) of 0.0175, resulting in a lift-to-drag ratio (Cl/Cd) of 28.00. In comparison, the dimpled wing generated a slightly lower Cl of 0.48, reflecting a 2.04% reduction in lift, and a marginally higher Cd of 0.0179, indicating a 2.29% increase in drag. These changes led to a reduction in aerodynamic efficiency, with the Cl/Cd ratio decreasing by 4.21% to a value of 26.82.

This reduction in aerodynamic efficiency for the dimpled wing at low AoA can be explained by the changes in near wall flow field conditions. Wall shear stress (Figure 6 (a) and (b)) and Q-criterion plots (Figure 7 (a) and (b)) revealed that the introduction of dimples triggered early transition of the boundary layer, turning the otherwise laminar attached flow into a turbulent flow. This artificially introduced turbulence increases skin

friction drag and disrupts the smooth pressure recovery over the airfoil surface. Consequently, although the flow remains attached, the aerodynamic performance deteriorates due to premature degradation of the boundary layer's favorable characteristics, even at a relatively low angle of attack.

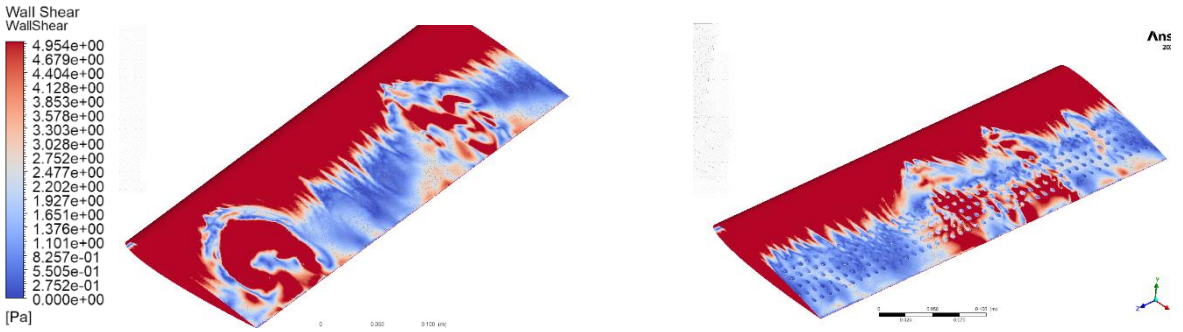

(a) (b)

Figure 8. Wall Shear at AoA $\mathbf{10}^0$ (a) Clean Wing (b) Dimpled Wing

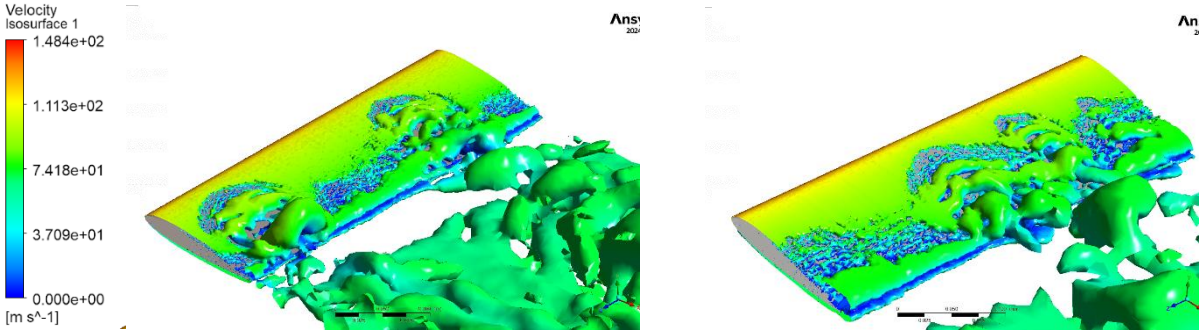

(a) (b)

Figure 9. Q Criterion Iso-surface at AoA $\mathbf{10}^0$ (a) Clean Wing (b) Dimpled Wing

At an angle of attack of 10°, the clean wing produced a lift coefficient (Cl) of 0.84 and a drag coefficient (Cd) of 0.0489, resulting in a lift-to-drag ratio (Cl/Cd) of 17.17. In contrast, the dimpled configuration achieved a higher Cl of 0.86, reflecting a 2.38% increase in lift, and a lower Cd of 0.0415, indicating a 15.14% reduction in drag. These improvements enhanced the aerodynamic efficiency, increasing the Cl/Cd ratio by 20.66% to a value of 20.72.

This performance gain can be attributed to the effect of dimples in energizing the boundary layer. The flow field visualizations using Q-criterion (Figure 9 (a) and (b)) revealed increased vortex activity in the turbulent boundary layer over the dimpled surface. These streamwise vortices introduced by the dimples enhanced momentum exchange, allowing the flow to remain attached for a longer portion of the chord. As a result, both lift enhancement and drag reduction were observed at this higher angle of attack.

Aerocoustic Performance

To evaluate the acoustic performance, a directivity analysis was conducted using a circular array of receivers positioned at a radius of 0.5 m from the trailing edge, located on the mid-span plane (half-chord spanwise location). Receivers were placed at 15° intervals around the full 360° circle for both 5° and 10° angle of attack. The Overall Sound Pressure Level (OASPL) was recorded at each receiver location and presented in the form of polar plots to visualize the noise directivity pattern for each case.

In addition to the directivity analysis, spectral analysis was performed at a representative receiver location. Sound Pressure Level (SPL) versus frequency plots were generated for both the clean and dimpled wing configurations at AoA = 5° and AoA = 10°, allowing comparison of the tonal and broadband noise characteristics resulting from the surface modifications.

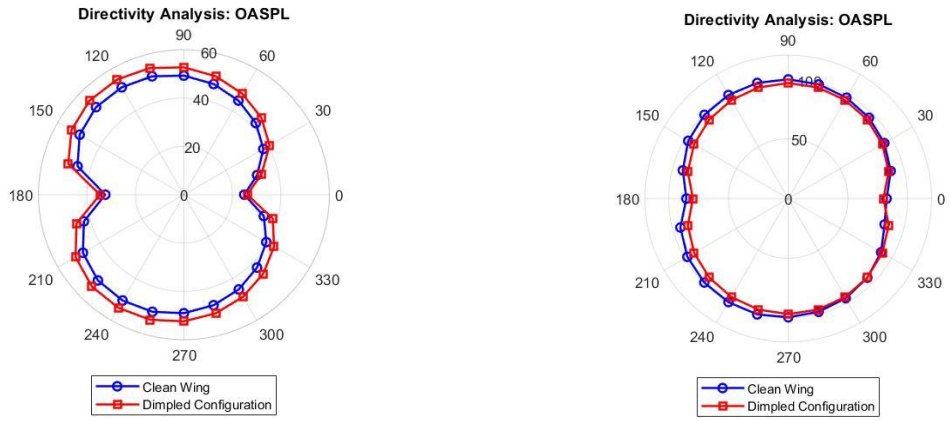

(a) (b)

Figure 10. Directivity Analysis for (a) AoA 5° (b) AoA 10°

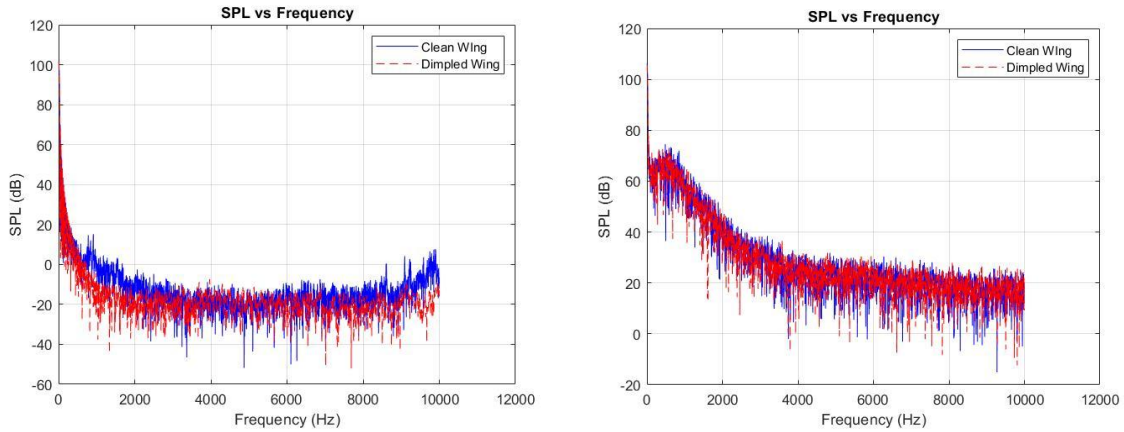

(a) (b)

Figure 11. Frequency Spectral Analysis (a) AoA 5° (b) AoA 10°

At an angle of attack of 5°, the dimpled wing configuration exhibited a slight increase in OASPL compared to the clean wing, with differences of approximately 1–2 dB observed around the receiver circle as shown in Figure 10(a). This increase is attributed to the additional turbulence and small-scale vortical structures introduced by the dimples, as evident from the flow field.

Spectral analysis revealed that the rise in SPL was primarily shifted to the 4000Hz-7000hz frequency range as illustrated in Figure 11(a). These high-frequency components had very low amplitudes and are expected to dissipate quickly in the far field, contributing minimally to perceived noise levels. The low-frequency region of the spectrum, which has a greater impact on far-field acoustic propagation, remained largely unaffected. In fact, certain frequencies like 1000Hz- 3000Hz showed slight reductions in SPL, indicating that the dimpled surface did not significantly degrade the overall acoustic behavior at this low angle of attack.

At an angle of attack of 10°, the dimpled configuration demonstrated a clear improvement in acoustic performance. The OASPL directivity plots showed a reduction of approximately 2–6 dB across most receiver positions compared to the clean wing (Figure 10(b)). This indicates a significant decrease in overall radiated noise due to the presence of dimples.

From a flow physics perspective, this reduction can be attributed to the influence of dimples on the boundary layer behavior under near-stall conditions. The dimples controlled streamwise vortices and enhance turbulent mixing within the boundary layer, which delays separation and stabilizes the flow over the trailing edge region. As a result, the intensity and irregularity of large-scale turbulent structures which are major sources of broadband noise are reduced, leading to lower sound emission.

In the frequency spectrum, no major shift in the trend or dominant frequency components was observed.

However, a general reduction in SPL magnitude across the entire spectrum was noted for the dimpled configuration as can be seen from Figure 11(b). This suggests that while the noise generation mechanisms remained similar, the overall acoustic energy radiated by the airfoil was reduced due to the modified and more organized flow field enabled by the surface dimples.

CONCLUSION

This study investigated the potential of dimpled surface configurations to enhance the aerodynamic and aeroacoustic performance of airfoils under low-speed flow conditions relevant to applications such as UAVs and small-scale wind turbines. Using high-fidelity CFD simulations with a DES turbulence model and the Ffowcs Williams–Hawkings acoustic analogy, the NACA 0012 airfoil was evaluated in both clean and dimpled configurations at angle of attack 5° and 10°.

Aerodynamically, the dimpled surface showed a minor performance penalty at 5° due to early boundary layer transition, increasing drag and reducing lift slightly. However, at 10°, the dimples delayed separation by energizing the boundary layer through enhanced vortex activity, resulting in both lift improvement and drag reduction. This led to a higher aerodynamic efficiency (Cl/Cd) compared to the clean configuration.

From an aeroacoustic perspective, the dimpled surface led to a slight increase in high-frequency noise at 5°, but with low SPL magnitudes that are expected to decay quickly in the far field. At 10°, a substantial reduction in OASPL ranging from 2–6 dB was observed in the directivity pattern, along with a general decrease in SPL across the spectrum. This reduction in radiated noise is attributed to the dimples' ability to suppress large-scale turbulent structures near the trailing edge under near-stall conditions.

Overall, the results demonstrate that properly configured dimples can offer dual benefits: improved aerodynamic performance at higher angle of attack and notable noise reduction, without requiring major structural changes. These findings highlight the potential of passive dimpled surface treatments as an effective design strategy for low-noise, high-lift airfoil applications.

ACKNOWLEDGEMENT

This project was funded by Senate Research Committee (SRC) grant of University of Moratuwa, Sri Lanka (Grant no: SRC/LT/2021/26)

REFERENCES

[1] B. Al Tlua, J. Rocha, Experimental investigation of NACA-0012 airfoil instability noise with sawtooth trailing edges, Wind Eng. (2021). https://doi.org/10.1177/0309524x211060548

[2] S. Ananthan, J. Sitaraman, N. Hariharan, Effect of shallow dimples on the aerodynamic performance of a symmetric airfoil, Aerospace 9 (2022) 1–15.

[3] J. Chen, L. Wu, T. Zhang, Aeroacoustic performance of various surface dimple configurations, AIAA J. 57 (2019) 4560–4572. https://doi.org/10.2514/1.J058070

[4] H. Choi, W.-P. Jeon, J. Kim, Control of flow over a bluff body, Annu. Rev. Fluid Mech. 40 (2008) 113–139. https://doi.org/10.1146/annurev.fluid.39.050905.110215

[5] Y. Choi, K. Kwon, D. Lee, Aerodynamic performance of airfoils with surface dimples at low Reynolds numbers, AIAA J. 52 (2014) 1212–1223. https://doi.org/10.2514/1.J052571

[6] Environmental Protection Agency, Guidelines for wind energy noise, 2020.

[7] B. Etter, Numerical investigation of dimpled surfaces for drag reduction, Master's thesis, University of Illinois, 2007.

[8] C. L. Etter, Comparative study of spherical and non-spherical dimples for flow control, Experiments in Fluids 61 (2020). https://doi.org/10.1007/s00348-020-02994-3

[9] Federal Aviation Administration, Noise exposure map guidelines, 2023.

[10] J. E. Ffowcs Williams, D. L. Hawkings, Sound generation by turbulence and surfaces in arbitrary motion, Philos. Trans.

R. Soc. Lond. A 264 (1969) 321–342. https://doi.org/10.1098/rsta.1969.0031

[11] M. Fouatih, K. Khellil, F. Chabane, Numerical investigation of vortex generators in enhancing airfoil performance, Renew. Energy 92 (2016) 335–346.

[12] M. S. Genç, U. Kaynak, Y. S. Uslu, Aerodynamic performance of passive flow control devices on airfoils, Aerospace Sci. Technol. 98 (2020) 105679.

[13] C. R. Kight, J. P. Swaddle, How and why environmental noise impacts animals: An integrative, mechanistic review, Ecol. Lett. 14 (2011) 1052–1061.

[14] S. Panda, H. V. Warrior, Flow control using shallow dimples at low Reynolds number, J. Fluids Eng. 143 (2021) 031202.

[15] R. E. Sheldahl, P. C. Klimas, Aerodynamic characteristics of seven symmetrical airfoil sections through 180-degree angle of attack for use in aerodynamic analysis of vertical axis wind turbines, 1981. https://doi.org/10.2172/6548367

[16] P. R. Spalart, S. Deck, M. L. Shur, K. D. Squires, M. K. Strelets, A. Travin, A new version of detached-eddy simulation, resistant to ambiguous grid densities, Theor. Comput. Fluid Dyn. 20 (2019) 181–195.

[17] L. Van Campenhout, J. Lefebvre, M. Brossard, Experimental investigation of dimple geometries on airfoil aerodynamics, J. Fluids Eng. 143 (2021). https://doi.org/10.1115/1.4048536

[18] S. Kumar, S. K. Singh, S. Jha, K. Baskaran, K. Srinivasan, S. Narayanan, On the reductions of airfoil broadband noise through circular dimples, Appl. Acoust. 217 (2024) 109819. https://doi.org/10.1016/j.apacoust.2023.109819

[19] C. L. Perry, Mitigation of Aeroacoustic Noise of a Fixed Wing Using Passive Flow Control, Georgia Southern Commons, 2023. https://digitalcommons.georgiasouthern.edu/etd/2632

[20] D. Moreau, L. Brooks, C. Doolan, Experimental investigation of flat plate self-noise reduction usingtrailing edge serrations, 2012. https://www.icas.org/icas_archive/ICAS2012/PAPERS/221.PDF

[21] T. Brooks, D. Stuart, M. Marcolini, NASA Reference Publication 1218 Airfoil Self-Noise and Prediction, 1989. https://ntrs.nasa.gov/api/citations/19890016302/downloads/19890016302.pdf